MedChemComm

A Zwitterionic Near-infrared Dye Linked TrkC Targeting Agent for Imaging Metastatic Breast Cancer

Journal:	*MedChemComm*
Manuscript ID	MD-RES-04-2018-000190.R2
Article Type:	Research Article
Date Submitted by the Author:	24-Jul-2018
Complete List of Authors:	Yang, Zhen; Houston Methodist Research Institute, Usama , Syed Muhammad; Texas A & M University, Department of Chemistry Li, Feng; Houston Methodist Research Institute Burgess, K.; Texas A&M University Department of Biochemistry and Biophysics, Li, Zheng; Houston Methodist Research Institute, Dept. of Translational Imaging

A Zwitterionic Near-infrared Dye Linked TrkC Targeting Agent for Imaging Metastatic Breast Cancer

Zhen Yang[1,3], Syed Muhammad Usama[2,3], Feng Li[1], Kevin Burgess*[2] and Zheng Li[1]*

[1] Center for Bioenergetics, Houston Methodist Research Institute, Houston, TX 77030, USA

[2] Department of Chemistry, Texas A & M University, Box 30012, College Station, TX 77842, USA

[3] Both authors contributed equally to this work

E-mail: burgess@tamu.edu; zli@houstonmethodist.org

ABSTRACT

Much effort has been devoted to targeting agents for imaging and chemotherapy of tumors in cancer research, but there remains significant unmet needs in that area. We have reported a series of preclinical TrkC targeting agents for diagnoses and treatment of metastatic breast cancer; however, with respect to optical imaging, there are limitations to the agents already disclosed. In this work, a TrkC targeting fragment was equipped with a zwitterionic cyanine dye to give a near-infrared probe for *in vivo* imaging of metastatic breast tumors, with excitation and emission wavelengths of 760 and 780 nm, respectively, and facilitated the aqueous dissolution of the final design. To our delight, the newly developed probe maintained the specific targeting to $TrkC^+$ 4T1 metastatic breast tumor cells as well as $TrkC^+$ metastatic breast tumor tissue. Upon

injection into 4T1-tumor-bearing mice, the tumor was visualized *in vivo* and *ex vivo* through the fluorescent signal of the probe. These data seem encouraging for further investigations toward developing a TrkC targeting agent for diagnosis of metastatic breast tumors.

INTRODUCTION

Development of imaging probes that selectively associate with metastatic tumor cells expands useful diagnostic tools for the therapeutic assessment of the cancer treatment.[1, 2] For the breast cancer, there is an emerging demand for imaging probes that are capable for the recognition of *metastatic*, not just normal, breast tumor cells.[3, 4] Tropomycin kinase receptor C (TrkC) has been identified as a characteristic regulator of breast cancer cell growth and metastasis and tends to be overexpressed in metastatic breast tumor cells.[5, 6] Consequently, it is a potential targets for active targeting of metastatic breast cancer.

Most often, monoclonal antibodies (mAbs) are used as targeting agents.[7, 8] Small-molecule alternatives, however, have advantages with respect to cost, reagent stabilities, immunogenic effects, circulation times in the course of patient imaging, and, most important superior permeation into solid tumors.[1, 9] Consequently, the focus of our research is on small molecules for active targeting of TrkC.

Targeting TrkC with small molecules has featured a bivalent targeting fragment (IY-IY, blue color throughout diagrams in this paper).[10-12] In this work, that fragment, "IY-IY", was covalently linked to a zwitterionic cyanine dye (purple color throughout) to give a near-infrared probe for TrkC targeted imaging. Polar, zwitterionic characteristics of the dye were anticipated to foster the aqueous dissolution for *in vivo* administration, and simultaneously diminish net-

charges that might otherwise induce non-specific binding.[13] Since the intrinsic structure of IY-IY fragment was preserved, we hypothesized that final assembly of the probe would maintain its characteristics of TrkC targeting.

RESULTS AND DISCUSSION

Probe Design

Motivation for these studies came from positive results obtained in a study of the photodynamic therapy (PDT) agent **A** in mice impregnated with 4T1 mouse breast tumors.[14] In that work, one single 10 mg/Kg dose followed by illumination for 10 min caused near complete regression of the primary tumor over 28 days *and* inhibited metastatic spread relative to untreated control animals.

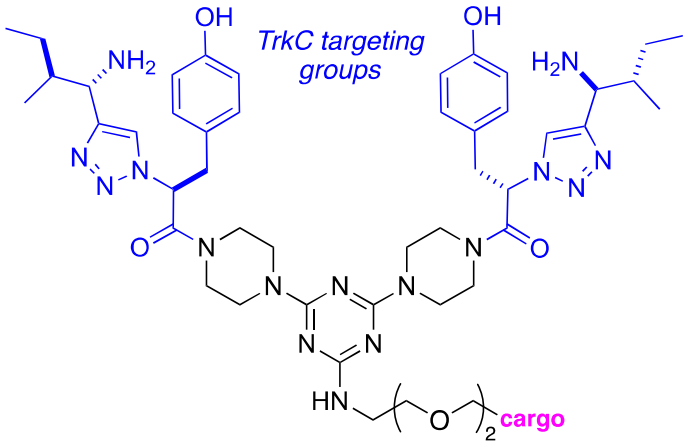

cargo =

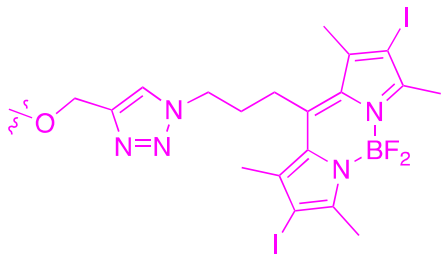

A
PDT agent

The next step in our research was to develop a TrkC-targeted compound for optical imaging *in vivo*. Agent **A**, and especially its non-iodinated analog, stained 4T1 cells (that are $TrkC^+$) well in culture,[15] but it is unsuitable for *in vivo* imaging because it absorbs light maximally at 530 nm. Dyes that absorb above 750 nm are preferred for *in vivo* imaging because tissue is most permeable to light above that wavelength, hence the fluors can be excited in more deeply situated tumors. Consequently, we designed and studied agent **B** which contains a aza-BODIPY.[16, 17]

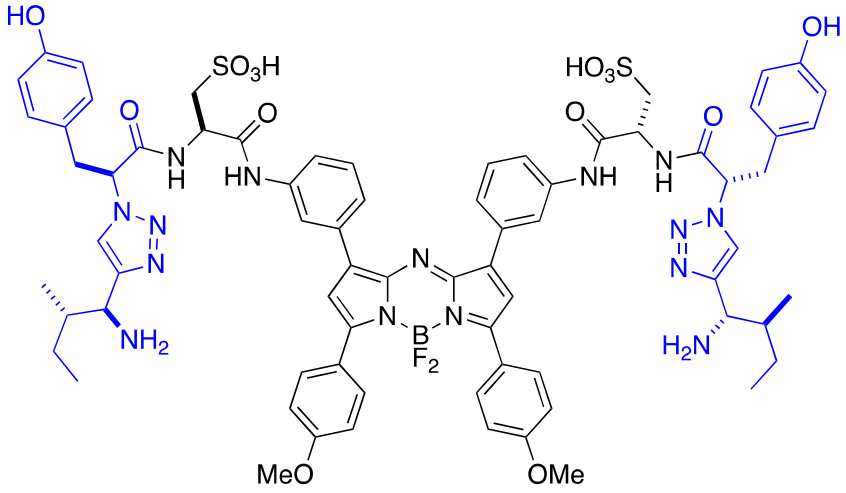

B
in vivo imaging
λ_{max} *633 nm*

The outcome of our studies on **B** were a mixed success.[10] Agent **B** selectively accumulated in the $TrkC^+$ 4T1 tumors (relative to an isomeric, non-TrkC targeting, control similar to that shown below). That observation means that the different linker and spacing of the TrkC-targeting groups in **B** relative to **A** did not perturb its honing ability; other work has shown that is not always the case.[18] On the other hand, a shortcoming was that **B** absorbs at 633 nm which, though more appropriate than 540 nm in **A**, is still not a long enough wavelength.

Another shortcoming was that **B** accumulated about three times more in the liver than in the tumor, and it had a long residence time there (still observed after 48 h).

Based on the studies outlined above, the current study was initiated to change the fluor completely, to a hydrophilic cyanine dye as in **1**. Structure **1** has the same IY-IY targeting arrangement as our original lead **A**, and a more water-soluble fluor than **B** that absorbs light maximally at around 760 nm. Consequently, the visibility of this probe *in vivo* should be superior to **A** and **B**, and we anticipated that it would be less retained in the liver than the lipophilic azaBODIPY system **B**. The parameter that could not be anticipated was the effect of the targeting groups in **1** offset by the pharmacokinetic influence of the cyanine fragment. Important work, particularly by Henary and co-workers, on distribution of cyanine dyes *in vivo* enables some predictions to be made with more confidence,[19-24] but, nevertheless, experimentation is necessary.

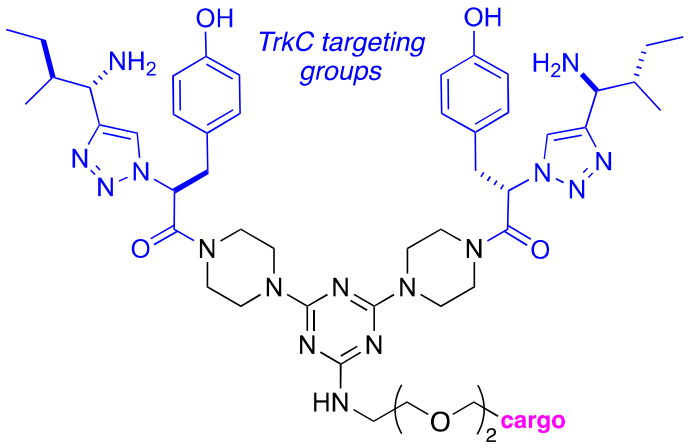

cargo =

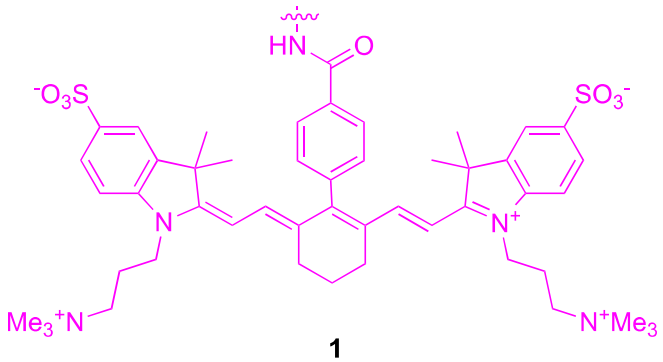

1

Probe Synthesis and Optical Properties

The IY-IY targeting group has been made many times previously in these labs, but for the current study an improved procedure was developed to facilitate synthesis on a larger scale. Details of the modified route are given in the supporting material, and the concept is outlined in Scheme 1. The last step involved a coupling of the targeting fragment **C** with the activated cyanine part **D**.[25] The innovation in the modification was in the construction of **C**. Previously IY-piperazine fragments had been added to the triazine, but that step did not scale well. Instead, the current route involves S*N*Ar reaction of tyrosine-derived azide, then click reaction to build up the IY-IY fragment in layers.

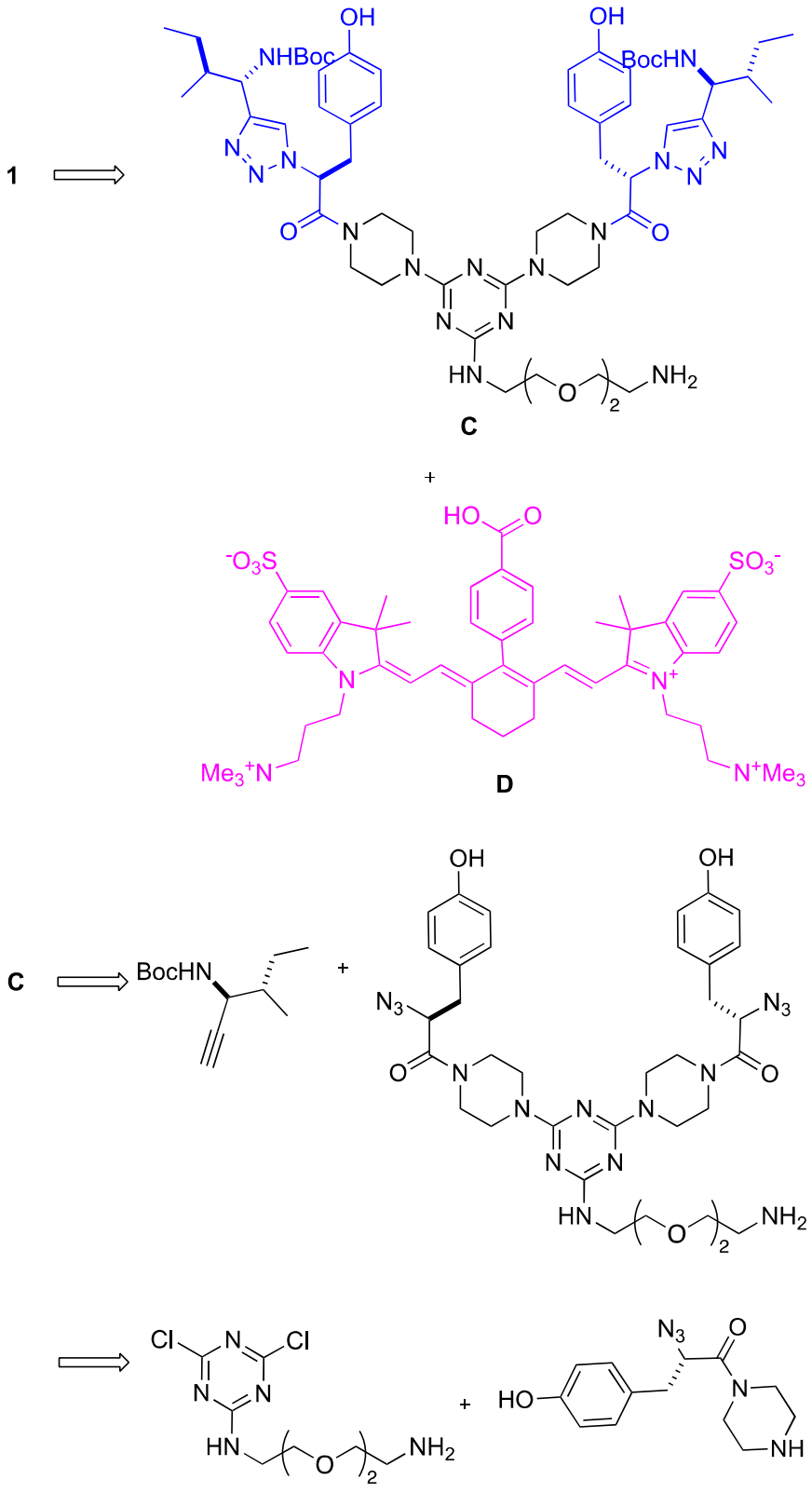

Scheme 1. Retrosynthetic route to probe **1** illustrating an improved route to the IY-IY fragment.

The following electronic spectral data summarize the key points from the full analysis shown in the supporting. Probe **1** had an extinction coefficient of 140,000 L mol^{-1} cm^{-1} and a quantum yield of 5.6% (in 7.4 PBS buffer); these data are typical of the strong absorption from the cyanine fragment and indicate an excellent overall brightness. Maximal absorption and emission were observed at 760 and 780 nm (in 7.4 PBS buffer), ideal for optical imaging.

Compound **2** is an isomer of **1** with the targeting amino acids inverted (YI-YI); this was a useful control in the cellular studies that are now described.

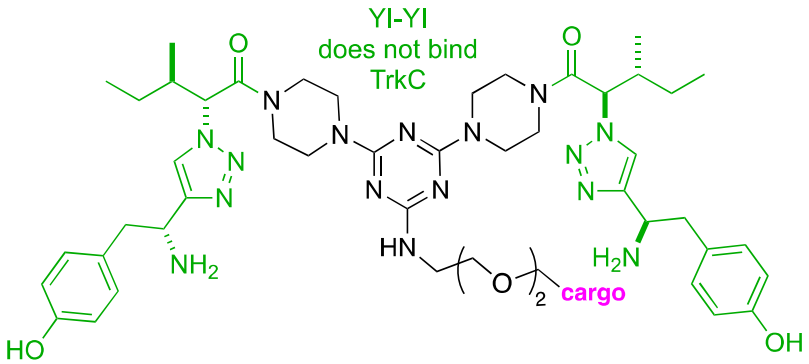

cargo =

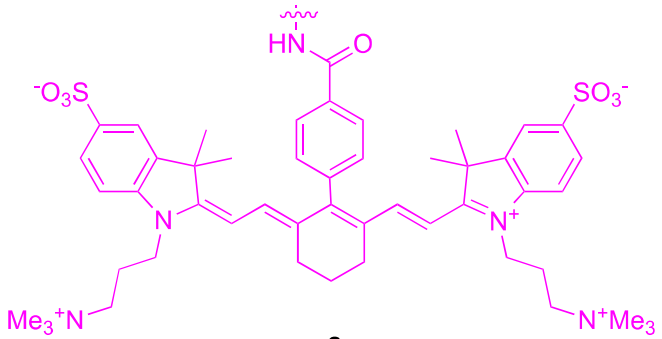

2

Probe Behavior in Live Cell and Tissue Studies

Probe **1** was first tested for binding cells stably transfected with TrkC; data obtained (Figure 1a, horizontal row) show the cells did, in fact, bind the probe, whereas the parent NIH 3T3 cells that do not express this receptor did not (Fig. 1b). Control experiments (Supporting Fig. S1-3),

demonstrated that the control probe **2** did not stain TrkC^{+} or wild type (TrkC^{-}) NIH 3T3 cells, and neither did the parent cyanine dye without the targeting group. Confocal studies at a higher magnification revealed **1** tends to localize in the lysosomes (Fig. 1c and d), just as natural neurotrophins to when they are imported via the TrkC receptor.[26] In histology studies with commercial samples from breast cancer patients, metastatic breast cancer tissue was stained but not normal tissue (Fig. 1e and f).

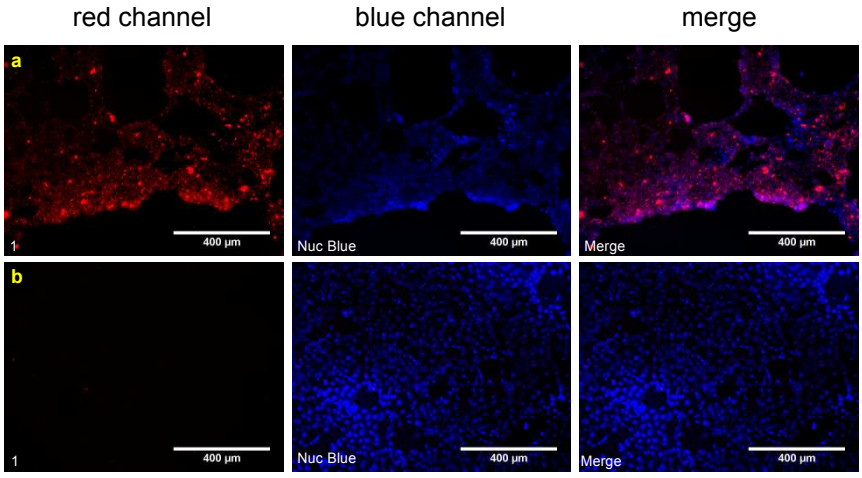

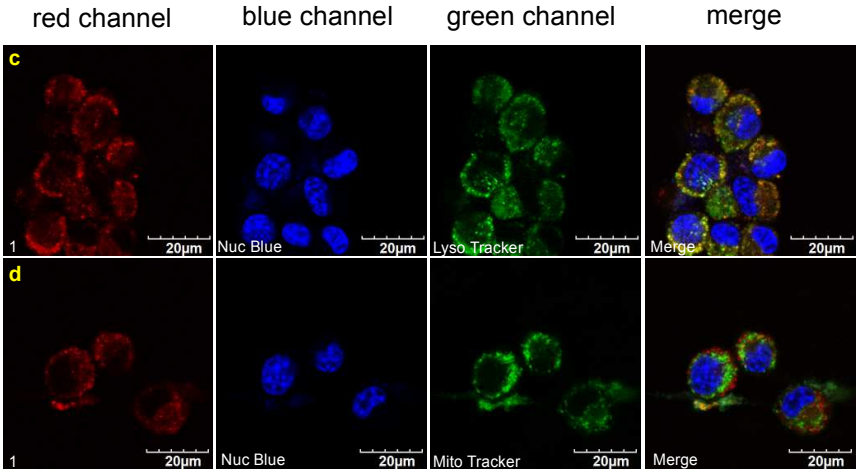

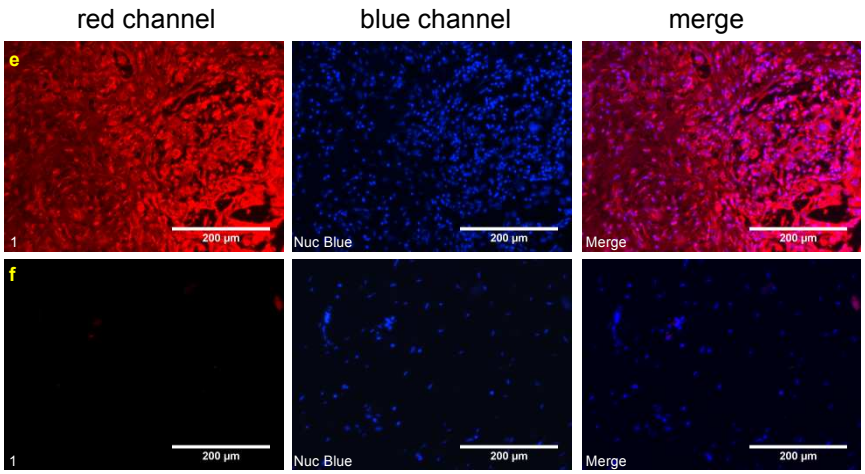

Figure 1. a Probe **1** binds NIH3T3 TrkC^{+} cells, but not to NIH3T3 WT cells (**b**). Confocal experiments revealed **1** colocalizes: **c** with LysoTracker Green; and, **d** not with MitoTracker Green. Histology studies of **1** with: **e** metastatic breast cancer tissue (invasive ductal carcinoma); and, **f** normal breast tissue (adjacent normal breast tissue). Throughout the blue channel is to detect nuclear staining with Nuc Blue.

In Vivo Imaging with Probe **1**

Mouse 4T1 breast tumor is a well-established animal model for study of human metastatic breast cancer.[27] In this study, murine 4T1 tumor cells were subcutaneously injected into BALB/c nu/nu mice to create 8-10 mm diameter metastatic breast tumor xenografts. After intravenous injection of the imaging probe, NIR fluorescence images of the tumor-bearing mice were captured at various time points after injection of **1** (Fig. 2). The 4T1 tumors were clearly visualized through the fluorescence differences displayed from tumor to muscle background as early as 15 min post injection of the targeting agent. Moreover, the agent **1** rapidly cleared from the body;

fluorescence intensities of the tumor dropped from 15 min to 1 h, and further at 3 h, and almost to background at 24 h. Compared to TrkC targeting agent **B**, the retention time of the **1** was much shorter, presumably because of the more hydrophilic nature of the zwitterionic dye.

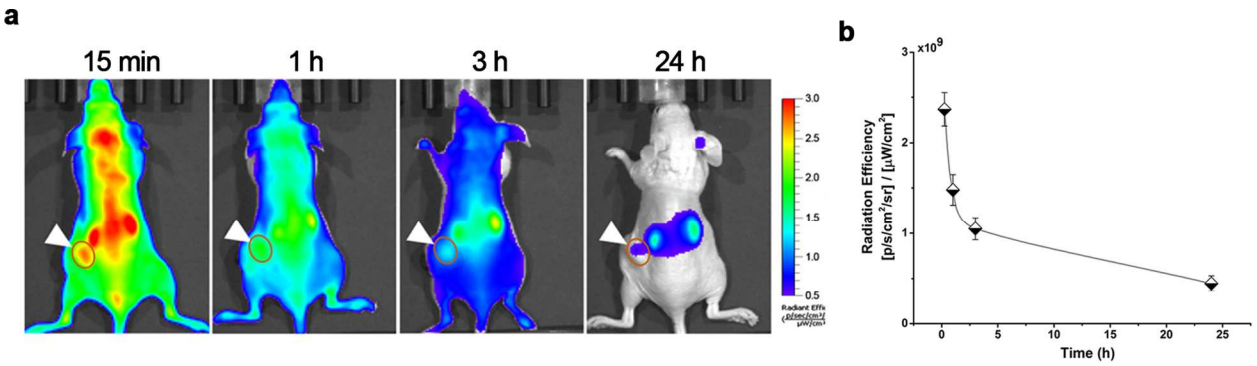

Figure 2. a *In vivo* NIR fluorescence images of 4T1 tumor-bearing mice at 15 min, 1 h, 3 h, and 24 h post-injection of the targeting agent. White arrows in indicate the tumors, and the circles mark ROI study of tumor for the quantification analysis in **b**. **b** Quantification of fluorescence in the tumors. Data shown represent mean ± SD (n = 3 per group).

To further validate tumor uptake of the targeting agent, internal organs of the imaged mice were collected for *ex vivo* imaging. The relatively higher fluorescence intensities displayed in tumors, compared to muscle background, indicated the selective update of the targeting agent by the tumors (Figure 3a). Trk receptors play important roles in the mammalian nervous system, and tends to exhibit high expression of TrkC receptor;[28, 29] however, we did not observe uptake in the mice brain and spinal cord, hence it appears that the size and charge of the probe suppress its penetration into the central nervous system. A kinetic curve of the tumor uptake extracted from *ex vivo* imaging data corresponded to that from *in vivo* imaging (Figure 3b). Uptake of the targeting agent in tumor reached its peak half an hour after the injection, then clearance from the body dominated.

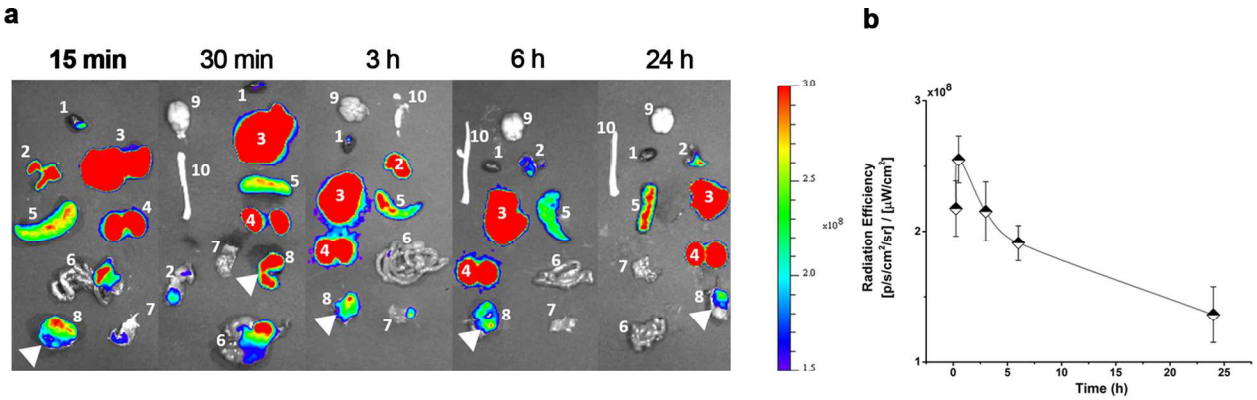

Figure 3. a Representative *ex vivo* fluorescence images of: 1 heart, 2 lung, 3 liver, 4 kidney, 5 spleen, 6 gastrointestine, 7 muscle, 8 tumor, 9 brain, 10 spinal cord, collected from the mice at 15min, 30 min, 3 h, 6 h and 24 h post-injection of the targeting agent. White arrows mark the tumors. **b** Quantification of fluorescence in the tumors. Data shown represent mean ± SD (n = 3 per group).

Probe **1** localized in TrkC expressing tumors, as anticipated, providing a way to stain them with NIR fluorescence. In retrospect, the observation that the probe was washed out of the system relatively rapidly can be attributed to the polarity of the cyanine dye. However, observation of rapid washout from tumors *in vivo* surprised us, for two reasons. First, the cell imaging data in this paper prove that the probe **1** is selectively imported into $TrkC^+$ cells. Secondly, at least some members of the parent dye system **E** (particularly where R^1 and R^2 contain carboxylate or sulfonate functionalities) tend to localize in many types of solid tumors[2, 30-32]. Further experiments are in progress to try to understand these apparent inconsistences.

CONCLUSIONS

In this work, an imaging probe that incorporated with TrkC targeting agent and zwitterionic NIR dye was reported for imaging metastatic breast cancer. *In vitro* and *in vivo* imaging studies showed the specific association of the TrkC targeting probe with 4T1 tumors. This study is

helpful for further development of TrkC targeting agent for theranostics of metastatic breast cancer.

MATERIALS AND METHODS

Probe synthesis

All reactions were carried out under an inert atmosphere (nitrogen or argon where stated) with dry solvents under anhydrous conditions. Glassware for anhydrous reactions was dried in an oven at 140 ºC for minimum 6 h prior to use. Dry solvents were obtained by passing the previously degassed solvents through activated alumina columns. Yields refer to chromatographically and spectroscopically (1H-NMR) homogeneous materials, unless otherwise stated. Reagents were purchased at a high commercial quality (typically 97 % or higher) and used without further purification, unless otherwise stated. Analytical thin layer chromatography (TLC) was carried out on Merck silica gel plates with QF-254 indicator and visualized by UV. Flash column chromatography was performed using silica gel 60 (Silicycle, 230-400 mesh). 1H and 13C spectra were recorded on a 400 MHz spectrometer and were calibrated using residual non-deuterated solvent as an internal reference. Detailed synthesis information is provided in supporting materials. The abbreviations or combinations in the supporting materials thereof were used to explain the multiplicities: s = singlet, d = doublet, t = triplet, q = quartet, m = multiplet, dd = doublet of doublet, ddd = doublet of doublet of doublets.

In-Vitro Assays

NIH3T3-WT cells (from American Type Culture Collection) were cultured on 75 cm2 culture flasks in Dulbecco's Modified Eagle Medium/nutrient mixture F-12 (DMEM/F12, Sigma Chemical, St. Louis, MO) supplemented with 10 % FBS. NIH3T3-TrkC cells were obtained and

cultured according to previous procedures1. Cells were cultured in a humidified incubator at 37 °C with 5 % CO2 and 95 % air.

Fluorescence microscopy

Intracellular localization of the NIH3T3 cells was measured using Olympus Fluoview FV1000. The images were taken at 60x/1.20 water immersed ojective. Lysosome staining Lysotracker Green DND 26 (Thermofisher), Mitochondria staining Mitotracker Green FM (Thermofisher) and for Nucleus, Nuc Blue ((Thermofisher) was used. 488 nm laser was used for green channel dyes, 205 nm laser was used for nucleus and 633 nm laser was used for 1 and 2. Rest of the Flourescence images were taken using Evos FL Imaging System (Thermofisher).

Intracellular localization

NIH3T3 cells were incubated with 20 μM for 2 hrs. at 37 oC. After 2 hrs, the cells were washed with PBS and LysoTracker and Mitotracker were added for 40 mins. The cells were washed again with PBS and nucleus was stained using Nuc Blue.

Histology on patient's tissues

Slide of human malignant melanoma tissue microarray (BR243w) was purchased from US Biomax, Inc., the array includes 13 cases of malignant melanoma and 12 cases of adjacent normal cells. The slide was transferred to a xylene bath for 10 min and then rehydrated in two changes of fresh absolute ethanol for 7 min each. Excess liquid was shaken off and the slide was incubated in fresh 90%, 70 % ethanol then water for 7 min each. The slide was washed in two changed of PBS for 5 min each, then incubated with PBS containing 4 % BSA for 30 min. The tissues were rinsed with PBS and incubated again in two changed of PBS for 5 min each. Compound 1 solution in 4 % PBS/BSA was added to the slide and incubated overnight at 4 oC. The slide was rinsed twice in PBS, then in water (10 min each). Then the slide contained 1 was

mounted in permanent mounting media with DAPI (Vector) and incubated at 4 oC for 4 h. The tissues were imaged with an Evos FL Imaging System. Throughout, digital images were captured with a 20x/ 0.45 excitation at 730 nm for 1 and 405 nm for DAPI.

Animal model

Murine breast cancer 4T1 cells were obtained from American Type Culture Collection and cultured as protocol suggested, *i.e.* in Dulbecco's modified Eagle medium (DMEM) supplemented with 10% fetal bovine serum (FBS) at 37 ^{o}C in humidified atmosphere with 5% CO_2. Upon 80% confluence, cells were collected and suspended into PBS, and then subcutaneously injected into 6 weeks BALB/c nu/nu mouse (Charles River) at 2 x 10^6 cells per 100 μL per mouse. Then mice were fed for two weeks to allow tumor growth reaching to 8-10 mm for the imaging study. Animal procedures were performed according to a protocol approved by Animal Care and Use Committee of Houston Methodist Research Institute and in accordance with the NIH guidelines for the care and use of laboratory animals (NIH Publication No. 85-23 Rev. 1985).

In vivo and *ex vivo* fluorescence imaging

The fluorescence imaging was performed using IVIS200 imaging system, and quantified the ROI study by Living Imaging software (Xenogen, CA). Excitation and emission filters were set at 745 nm and 800 nm, respectively, for imaging acquisition. For injection, the synthesized agent was firstly prepared as 1 mM stock solution in DMSO, and then diluted into 10 nmol per 100 μL in PBS for each mouse. Upon intravenous injection via tail vein, the mice (3 per group) were anesthetized to allow imaging acquisition accomplished. As to *ex vivo* imaging, mice (3 per group) were euthanized as animal protocol described at various time points after injection of the

targeting agent, and internal organs (*i.e.* heart, lung, liver, kidney, spleen, gestrointestine, tumor, muscle, brain, spinal cord) were collected for *ex vivo* imaging acquisition. Upon the imaging acquisition, ROI analysis and quantification of the fluorescence signals were performed with Living Imaging software.

ASSOCIATED CONTENT

Supporting Information

Scheme and full details of compounds syntheses and characterizations and in vitro cell uptake study

AUTHOR INFORMATION

The authors declare no competing financial interests.

AKNOWLEDGEMENTS

We thank DoD BCRP Breakthrough Award (BC141561 and BC141561P1), CPRIT (RP150559 and RP170144), The Robert A. Welch Foundation (A-1121) and George and Angelina Kostas Research award for financial support. The NMR instrumentation at Texas A&M University was supported by a grant from the National Science Foundation (DBI-9970232) and the Texas A&M University System. The Olympus FV1000 confocal microscope acquisition was supported by the Office of the Vice President for Research at Texas A&M University. We thank the preclinical imaging core facility of Houston Methodist Research Institute for imaging support. Procedures for animal housing, maintenance, and euthanization were performed according to the American Veterinary Medical Association guidelines, and the IACUC approval from Methodist Hospital.

KEYWORDS

BODIPY, 4,4-difluoro-4-bora-3a,4a-diaza-s-indacene; NT3, neurotrophin-3; PET, positron emission tomography; Trk, Tropomyosin receptor kinases.

REFERENCES

1. C. S. Kue, A. Kamkaew, K. Burgess, L. V. Kiew, L. Y. Chung and H. B. Lee, *Medicinal Research Reviews*, 2016, **36**, 494-575.
2. M. Gao, F. Yu, C. Lv, J. Choo and L. Chen, *Chemical Society Reviews*, 2017, **46**, 2237-2271.
3. C. Cedolini, S. Bertozzi, A. P. Londero, S. Bernardi, L. Seriau, S. Concina, F. Cattin and A. Risaliti, *Clinical Breast Cancer*, 2014, **14**, 235-240.
4. H. G. Welch, D. H. Gorski and P. C. Albertsen, *New England Journal of Medicine*, 2015, **373**, 1685-1687.
5. W. Jin, G. M. Kim, M. S. Kim, M. H. Lim, C. Yun, J. Jeong, J.-S. Nam and S.-J. Kim, *Carcinogenesis*, 2010, **31**, 1939-1947.
6. A. Vaishnavi, A. T. Le and R. C. Doebele, *Cancer Discovery*, 2015, **5**, 25.
7. D. J. Slamon, B. Leyland-Jones, S. Shak, H. Fuchs, V. Paton, A. Bajamonde, T. Fleming, W. Eiermann, J. Wolter, M. Pegram, J. Baselga and L. Norton, *New England Journal of Medicine*, 2001, **344**, 783-792.
8. M. Ogawa, N. Kosaka, P. L. Choyke and H. Kobayashi, *Cancer Research*, 2009, **69**, 1268.
9. K. Imai and A. Takaoka, *Nature Reviews Cancer*, 2006, **6**, 714.
10. A. Kamkaew, F. Li, Z. Li and K. Burgess, *MedChemComm*, 2017, **8**, 1946-1952.
11. C. S. Kue, A. Kamkaew, H. B. Lee, L. Y. Chung, L. V. Kiew and K. Burgess, *Molecular Pharmaceutics*, 2015, **12**, 212-222.
12. A. Kamkaew and K. Burgess, *Journal of Medicinal Chemistry*, 2013, **56**, 7608-7614.
13. H. S. Choi, K. Nasr, S. Alyabyev, D. Feith, J. H. Lee, S. H. Kim, Y. Ashitate, H. Hyun, G. Patonay, L. Strekowski, M. Henary and J. V. Frangioni, *Angewandte Chemie International Edition*, 2011, **50**, 6258-6263.
14. S. C. Kue, Anyanee Kamkaew, Hong Boon Lee, Lip Long Chung, Lik Voon Kiew, and Kevin Burgess, *Mol. Pharmacetics*, 2015, **12**, 212-222.
15. A. Kamkaew and K. Burgess, *Chem. Comm.*, 2015, **51**, 10664-10667.
16. M. A. Pysz, S. S. Gambhir and J. K. Willmann, *Clin. Radiol.*, 2010, **65**, 500-516.
17. J. V. Frangioni, *Current Opinion in Chemical Biology*, 2003, **7**, 626-634.
18. A. Kamkaew, N. Fu, W. Cai and K. Burgess, *ACS Medicinal Chemistry Letters*, 2017, **8**, 179-184.
19. H.-S. Choi, K. Nasr, S. Alyabyev, D. Feith, J.-H. Lee, S.-H. Kim, Y. Ashitate, H. Hyun, G. Patonay, L. Strekowski, M. Henary and J. V. Frangioni, *Angewandte Chemie, International Edition*, 2011, **50**, 6258-6263.
20. G. Beckford, E. Owens, M. Henary and G. Patonay, *Talanta*, 2012, **92**, 45-52.
21. H. S. Choi, S. L. Gibbs, J. H. Lee, S. H. Kim, Y. Ashitate, F. Liu, H. Hyun, G. L. Park, Y. Xie, S. Bae, M. Henary and J. V. Frangioni, *Nat. Biotechnol.*, 2013, **31**, 148-153.

22. N. S. James, Y. Chen, P. Joshi, T. Y. Ohulchanskyy, M. Ethirajan, M. Henary, L. Strekowski and R. K. Pandey, *Theranostics*, 2013, **3**, 692-702, 611 pp.
23. E. A. Owens, H. Hyun, J. G. Tawney, H. S. Choi and M. Henary, *J. Med. Chem.*, 2015, **58**, 4348-4356.
24. C. N. Njiojob, E. A. Owens, L. Narayana, H. Hyun, H. S. Choi and M. Henary, *J. Med. Chem.*, 2015, **58**, 2845-2854.
25. D. Su, C. L. Teoh, A. Samanta, N.-Y. Kang, S.-J. Park and Y.-T. Chang, *Chem. Commun.* , 2015, **51**, 3989-3992.
26. R. Butowt and C. S. von Bartheld, *J. Neurosci.*, 2001, **21**, 8915-8930.
27. B. A. Pulaski and S. Ostrand-Rosenberg, in *Current Protocols in Immunology*, John Wiley & Sons, Inc., 2001, DOI: 10.1002/0471142735.im2002s39.
28. B. Stoleru, A. M. Popescu, D. E. Tache, O. M. Neamtu, G. Emami, L. G. Tataranu, A. S. Buteica, A. Dricu and S. O. Purcaru, *Mædica*, 2013, **8**, 43-48.
29. Y. Muragaki, N. Timothy, S. Leight, B. L. Hempstead, M. V. Chao, J. Q. Trojanowski and V. M. Y. Lee, *The Journal of Comparative Neurology*, 1995, **356**, 387-397.
30. X. Tan, S. F. Luo, D. F. Wang, Y. F. Su, T. F. Cheng and C. Shi, *Biomaterials*, 2012, **33**, 2230-2239.
31. S. Luo, X. Yang and C. Shi, *Curr Med Chem*, 2016, **23**, 483-497.
32. C. Zhang, T. Liu, Y. Su, Y. Zhu, X. Tan, S. Fan, L. Zhang, Y. Zhou, T. Cheng and C. Shi, *Biomaterials*, 2010, **31**, 6612-6617.

Table of Content

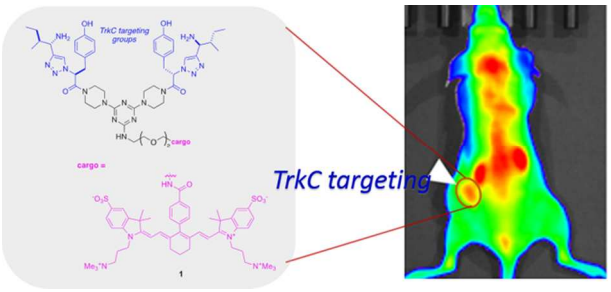

A probe that conjugated TrkC targeting agent with zwitterionic near-infrared dye was reported for imaging of metastatic breast cancer.